

# Determination of $U(1)_A$ restoration from pion and $a_0$ -meson screening masses: Toward the chiral regime

Masahiro Ishii,<sup>1,\*</sup> Koji Yonemura,<sup>1,†</sup> Junichi Takahashi,<sup>1,‡</sup> Hiroaki Kouno,<sup>2,§</sup> and Masanobu Yahiro<sup>1,¶</sup>

<sup>1</sup>*Department of Physics, Graduate School of Sciences, Kyushu University, Fukuoka 812-8581, Japan*

<sup>2</sup>*Department of Physics, Saga University, Saga 840-8502, Japan*

(Dated: October 1, 2018)

We incorporate the effective restoration of  $U(1)_A$  symmetry in the 2+1 flavor entanglement Polyakov-loop extended Nambu–Jona-Lasinio (EPNJL) model by introducing a temperature-dependent strength  $K(T)$  to the Kobayashi-Maskawa–t Hooft (KMT) determinant interaction.  $T$  dependence of  $K(T)$  is well determined from pion and  $a_0$ -meson screening masses obtained by lattice QCD (LQCD) simulations with improved p4 staggered fermions. The strength is strongly suppressed in the vicinity of the pseudocritical temperature of chiral transition. The EPNJL model with the  $K(T)$  well reproduces meson susceptibilities calculated by LQCD with domain-wall fermions. The model shows that the chiral transition is second order at the “light-quark chiral-limit” point where the light quark mass is zero and the strange quark mass is fixed at the physical value. This indicates that there exists a tricritical point. Hence the location is estimated.

PACS numbers: 11.30.Rd, 12.40.-y, 21.65.Qr, 25.75.Nq

## I. INTRODUCTION

Meson masses are important quantities to understand the properties of Quantum Chromodynamics (QCD) vacuum. For example, the difference between pion and sigma-meson masses is mainly originated in the spontaneous breaking of chiral symmetry, so that the restoration can be determined from temperature ( $T$ ) dependence of the mass difference. Similar analysis is possible for the effective restoration of  $U(1)_A$  symmetry through the difference between pion and  $a_0$ -meson (Lorentz scalar and isovector meson) masses.

$U(1)_A$  symmetry is explicitly broken by the axial anomaly and the current quark mass. In the effective model, the  $U(1)_A$  anomaly is simulated by the Kobayashi-Maskawa–t Hooft (KMT) determinant interaction [1, 2]. The coupling constant  $K$  of the KMT interaction is proportional to the instanton density screened by the medium with finite  $T$  [3]. Hence  $K$  becomes small as  $T$  increases:  $K = K(T)$ . Pisarski and Yaffe discussed the suppression  $S(T) \equiv K(T)/K(0)$  for high  $T$ , say  $T \gtrsim 2T_c$  for the pseudocritical temperature  $T_c$  of chiral transition, by calculating the Debye-type screening [3]:

$$\begin{aligned} S(T) &= \exp \left[ -\pi^2 \rho^2 T^2 \left( \frac{2}{3} N_c + \frac{1}{3} N_f \right) \right] \\ &= \exp[-T^2/b^2], \end{aligned} \quad (1)$$

where  $N_c$  ( $N_f$ ) is the number of colors (flavors) and the typical instanton radius  $\rho$  is about 1/3 fm, and hence the suppression parameter  $b$  is about  $0.70T_c$  for  $N_c = N_f = 3$  of our interest [4]; note that 2+1 flavor LQCD simulations show  $T_c = 154 \pm 9$  MeV [5–7]. This phenomenon is called “effective restoration of  $U(1)_A$  symmetry”, since  $U(1)_A$  symmetry

is always broken in the current-operator level but effectively restored at higher  $T$  in the vacuum expectation value.

Figure 1 shows the current status of knowledge on 2+1 flavor phase diagram for various values of light-quark mass  $m_l$  and strange-quark mass  $m_s$ . QCD shows a first-order phase transition associated with the breaking of chiral ( $Z_3$ ) symmetry at the lower left (upper right) corner [8, 9]. When  $m_l$  and  $m_s$  are finite, these first-order transitions become second order of 3d Ising ( $Z(2)$ ) universality class, as shown by the solid lines [8, 9].

However, the order of chiral transition and its universality class are unknown on the vertical line of  $m_l = 0$  and  $m_s > 0$ , and it is considered to be related to the effective  $U(1)_A$  restoration. In the two-flavor chiral limit of  $(m_l, m_s) = (0, \infty)$  at the upper left corner, for example, the order may be second order of  $O(4)$  class if the effective restoration is not completed at  $T = T_c$ , because the chiral symmetry becomes  $SU_L(2) \times SU_R(2)$  isomorphic to  $O(4)$  in the situation and the transition is then expected to be in the 3d  $O(4)$  universality class [8, 9]. When  $U(1)_A$  symmetry is restored completely at  $T = T_c$ , it was suggested in Ref. [8] that the chiral transition becomes the first order. Recently, however, it was pointed out in Ref. [10] that the second order is still possible. In this case, the universality class is not  $O(4)$  but  $U_L(2) \times U_R(2)$ . There are many lattice QCD (LQCD) simulations made so far to clarify the order and its universality class in the two-flavor chiral limit of  $(m_l, m_s) = (0, \infty)$  and the light-quark chiral limit where  $m_l$  vanishes with  $m_s$  fixed at the physical value, but these are still controversial; see Refs. [11–22] and therein.

Very recently, the effective restoration of  $U(1)_A$  symmetry was investigated by pion and  $a_0$ -meson screening masses calculated with LQCD with improved p4 staggered fermions [23] and also by meson susceptibilities calculated with LQCD with domain-wall fermions [24, 25]. The effective restoration of  $U(1)_A$  symmetry thus becomes an important current issue.

In LQCD, pole and screening masses are evaluated from the exponential decay of mesonic correlation functions in the temporal and spatial directions, respectively, but for finite  $T$

\*ishii@phys.kyushu-u.ac.jp

†yonemura@phys.kyushu-u.ac.jp

‡takahashi@phys.kyushu-u.ac.jp

§kounoh@cc.saga-u.ac.jp

¶yahiro@phys.kyushu-u.ac.jp

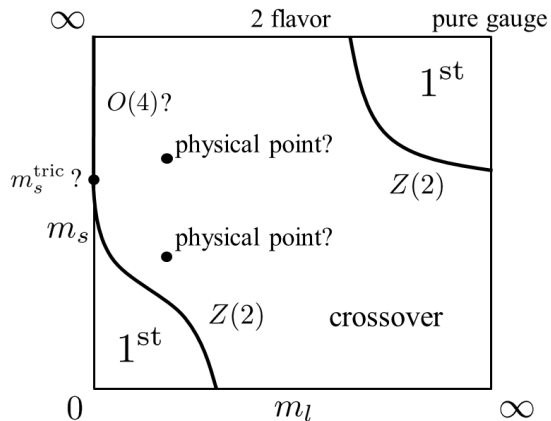


Fig. 1: A schematic phase diagram of 2+1 flavor QCD as a function of light-quark mass  $m_l$  and strange-quark mass  $m_s$ . A tricritical point is likely to appear on the  $m_s$  axis; the location is shown by  $(m_l, m_s) = (0, m_s^{\text{tric}})$ . The solid lines stand for second-order transitions belonging to the universality class labeled, where the labels  $Z(2)$  and  $O(4)$  mean the 3d Ising and the 3d  $O(4)$  class, respectively.

the lattice size is smaller in the temporal direction than in the spatial direction. This makes LQCD simulations less feasible for pole masses than for screening masses. The problem is getting serious as  $T$  increases. This is the reason why meson screening masses are calculated in most of LQCD simulations. In fact, as mentioned above, state-of-the-art LQCD calculations were done for meson screening masses with large volumes ( $16^3 \times 4$ ,  $24^3 \times 6$ ,  $32^3 \times 8$ ) in a wide range of  $T$  [23].

The effective model is suitable for qualitative understanding of QCD. In fact, the QCD phase diagram, the properties of light-meson pole masses and the  $T$  dependence of  $U(1)_A$  anomaly have been studied extensively with the Polyakov-loop extended Nambu–Jona-Lasinio (PNJL) model [26–41]. The PNJL model can treat the deconfinement and chiral transitions simultaneously, but cannot reproduce their coincidence seen in 2-flavor LQCD data, when the model parameters are properly set to reproduce  $T_c$  calculated with LQCD [32]. This problem is solved by introducing the four-quark vertex depending on the Polyakov-loop [42, 43]. The model with the entanglement vertex is referred to as the entanglement-PNJL (EPNJL) model. The EPNJL model is successful in reproducing the phase diagram in 2-flavor QCD at imaginary chemical potential [44, 45] and real isospin chemical potential [46], and well accounts for the phase diagram in the  $m_l$ – $m_s$  plane, i.e., the so-called Columbia plot in 2+1 flavor QCD [47]. So far,  $T$  dependence of  $U(1)_A$  anomaly and low-lying meson pole masses was studied extensively by both the PNJL and EPNJL models [29, 40, 41, 48], but  $T$  dependence of meson screening masses was investigated by the EPNJL model only in our previous work [49].

In NJL-type models, it is well known that the calculation of

meson screening mass  $M_{\xi, \text{scr}}$  is difficult, where  $\xi$  denotes the type of meson. In fact, only a few trials were made so far [50, 51]. The first problem is the regularization. The regularization widely used is the three-dimensional momentum cutoff, but it breaks Lorentz invariance at  $T = 0$  and spatial-translation invariance at any  $T$ . This generates unphysical oscillations in the spatial correlation function  $\eta_{\xi\xi}(r)$  [51]. This refuses us to determine  $M_{\xi, \text{scr}}$  from the asymptotic form of  $\eta_{\xi\xi}(r)$  as

$$M_{\xi, \text{scr}} = - \lim_{r \rightarrow \infty} \frac{d \ln \eta_{\xi\xi}(r)}{dr}. \quad (2)$$

This problem can be solved [51] by introducing the Lorentz-invariant Pauli-Villars (PV) regularization [52].

Even after the unphysical oscillations are removed, heavy numerical calculations are still required to obtain  $\eta_{\xi\xi}(r)$  at large  $r$  [51]. This is the second problem. In the model calculation, the spatial correlation function is obtained first in the momentum representation ( $\tilde{q} = \pm|\mathbf{q}|$ ) as  $\chi_{\xi\xi}(0, \tilde{q}^2)$ . Hence we have to make the Fourier transform from  $\chi_{\xi\xi}(0, \tilde{q}^2)$  to  $\eta_{\xi\xi}(r)$ :

$$\eta_{\xi\xi}(r) = \frac{1}{4\pi^2 i r} \int_{-\infty}^{\infty} d\tilde{q} \tilde{q} \chi_{\xi\xi}(0, \tilde{q}^2) e^{i\tilde{q}r}. \quad (3)$$

The  $\tilde{q}$  integration is quite hard particularly at large  $r$ , since the integrand consists of a slowly damping function  $\tilde{q} \chi_{\xi\xi}(0, \tilde{q}^2)$  and a highly oscillating function  $e^{i\tilde{q}r}$ . If  $\chi_{\xi\xi}(0, \tilde{q}^2)$  has a pole below the cut in the complex  $\tilde{q}$  plane, one can easily determine  $M_{\xi, \text{scr}}$  from the pole location. In the old formulation of Ref. [51], the condition was not satisfied, since logarithmic cuts appear in the vicinity of the real  $\tilde{q}$  axis in addition to physical cuts. Very recently we solved the problem in our previous paper [49], showing that the logarithmic cuts near the real  $\tilde{q}$  axis are unphysical and removable. In the new formulation based on the PV regularization, there is no logarithmic cut and a pole appears below physical cuts, as shown later.

In this paper, we incorporate the effective restoration of  $U(1)_A$  symmetry in the 2+1 flavor EPNJL model by introducing a  $T$ -dependent coupling strength  $K(T)$  to the KMT interaction.  $T$  dependence of  $K(T)$  is well determined from state-of-the-art 2+1 flavor LQCD results [23] on pion and  $a_0$ -meson screening masses. For the derivation of meson screening mass, we extend the previous prescription of Ref. [49] for 2 flavors to 2+1 flavors. The  $K(T)$  determined from the LQCD data is strongly suppressed near  $T_c$ . Using the parameter set, we show that the chiral transition is second order in the light-quark chiral limit. This result indicates that there exists a tricritical point near the “light-quark chiral-limit” point in the  $m_l$ – $m_s$  plane. We then estimate the location.

We recapitulate the EPNJL model and the method of calculating meson screening masses in Sec. II and show the results of numerical calculations in Sec. III. Section IV is devoted to a summary.

## II. MODEL SETTING

### A. EPNJL model

We start with the 2+1 flavor EPNJL model [42, 43]. The Lagrangian density is

$$\begin{aligned} \mathcal{L} = & \bar{\psi}(i\gamma_\nu D^\nu - \hat{m}_0)\psi + G_s(\Phi) \sum_{a=0}^8 [(\bar{\psi}\lambda_a\psi)^2 + (\bar{\psi}i\gamma_5\lambda_a\psi)^2] \\ & - K(T) \left[ \det_{f,f'} \bar{\psi}_f(1 + \gamma_5)\psi_{f'} + \det_{f,f'} \bar{\psi}_f(1 - \gamma_5)\psi_{f'} \right] \\ & - \mathcal{U}(\Phi[A], \bar{\Phi}[A], T) \end{aligned} \quad (4)$$

with quark fields  $\psi = (\psi_u, \psi_d, \psi_s)^T$  and  $D^\nu = \partial^\nu + iA^\nu$  with  $A^\nu = \delta_0^\nu g(A^0)_a t_a/2 = -\delta_0^\nu ig(A_4)_a t_a/2$  for the gauge coupling  $g$ , where the  $\lambda_a$  ( $t_a$ ) are the Gell-Mann matrices in flavor (color) space and  $\lambda_0 = \sqrt{2/3} \mathbf{I}$  for the unit matrix  $\mathbf{I}$  in flavor space. The determinant in (4) is taken in flavor space. For the 2+1 flavor system, the current quark masses  $\hat{m}_0 = \text{diag}(m_u, m_d, m_s)$  satisfy a relation  $m_s > m_l \equiv m_u = m_d$ . In the EPNJL model, the coupling strength  $G_s(\Phi)$  of the scalar-type four-quark interaction depends on the Polyakov loop  $\Phi$  and its Hermitian conjugate  $\bar{\Phi}$  as

$$G_s(\Phi) = G_s(0) [1 - \alpha_1 \Phi \bar{\Phi} - \alpha_2 (\Phi^3 + \bar{\Phi}^3)]. \quad (5)$$

This entanglement coupling is charge-conjugation and  $Z_3$  symmetric. When  $\alpha_1 = \alpha_2 = 0$ , the EPNJL model is reduced to the PNJL model. We set  $\alpha_2 = 0$  for simplicity, since the  $\alpha_2$  term yields the same effect as the  $\alpha_1$  term in the present analysis. As shown later in Sec. III, the value of  $\alpha_1$  is determined from LQCD data on pion and  $a_0$ -meson screening masses; the resulting value is  $\alpha_1 = 1.0$ .

For  $T$  dependence of  $K(T)$ , we assume the following form phenomenologically:

$$K(T) = \begin{cases} K(0) & (T < T_1) \\ K(0)e^{-(T-T_1)^2/b^2} & (T \geq T_1) \end{cases}. \quad (6)$$

For high  $T$  satisfying  $T \gg T_1$ , the form (6) is reduced to (1). As shown later in Sec. III, the values of  $T_1$  and  $b$  are well determined from LQCD data on pion and  $a_0$ -meson screening masses; the resulting values are  $T_1 = 0.79T_c = 121$  MeV and  $b = 0.23T_c = 36$  MeV.

After the Pisarski-Yaffe discussion on  $S(T)$ ,  $T$  dependence of the instanton density was estimated theoretically by the instanton-liquid model [4], but the estimation is applicable only for  $T \gtrsim 2T_c$ . For this reason, in Ref. [48], a Woods-Saxon form  $(1 + e^{(T-T'_1)/b'})^{-1}$  with two parameters  $T'_1$  and  $b'$  was used phenomenologically for  $K(T)/K(0)$ . The present form (6) has  $T$  dependence similar to the Woods-Saxon form.

In the EPNJL model, the time component of  $A_\mu$  is treated as a homogeneous and static background field, which is governed by the Polyakov-loop potential  $\mathcal{U}$ . In the Polyakov gauge,  $\Phi$  and  $\bar{\Phi}$  are obtained by

$$\Phi = \frac{1}{3} \text{tr}_c(L), \quad \bar{\Phi} = \frac{1}{3} \text{tr}_c(L^*) \quad (7)$$

with  $L = \exp[iA_4/T] = \exp[i\text{diag}(A_4^{11}, A_4^{22}, A_4^{33})/T]$  for real variables  $A_4^{jj}$  satisfying  $A_4^{11} + A_4^{22} + A_4^{33} = 0$ . For zero quark chemical potential where  $\Phi = \bar{\Phi}$ , one can set  $A_4^{33} = 0$  and determine the others as  $A_4^{22} = -A_4^{11} = \cos^{-1}[(3\Phi - 1)/2]$ .

We use the logarithm-type Polyakov-loop potential of Ref. [35] as  $\mathcal{U}$ . The parameter set in  $\mathcal{U}$  has already been determined from LQCD data at finite  $T$  in the pure gauge limit. The potential has a parameter  $T_0$  and yields a first-order deconfinement phase transition at  $T = T_0$ . The parameter used to be set to  $T_0 = 270$  MeV, since LQCD data show the phase transition at  $T = 270$  MeV in the pure gauge limit. In full QCD with dynamical quarks, however, the PNJL model with this value of  $T_0$  is found not to explain LQCD results. Nowadays,  $T_0$  is then rescaled to reproduce the LQCD results. In the present case, we take  $T_0 = 180$  MeV so that the EPNJL model can reproduce LQCD results for the pseudocritical temperature  $T_c^{\text{deconf}}$  of deconfinement transition; actually,  $T_c^{\text{deconf}} = 165$  MeV in the EPNJL model and  $170 \pm 7$  MeV in LQCD [53].

Making the mean field approximation (MFA) to (4) leads to the linearized Lagrangian density

$$\mathcal{L}^{\text{MFA}} = \bar{\psi}S^{-1}\psi - U_M - \mathcal{U}(\Phi[A], \bar{\Phi}[A], T) \quad (8)$$

with the quark propagator

$$S = (i\gamma_\nu \partial^\nu - \gamma_0 A^0 - \hat{M})^{-1}, \quad (9)$$

where  $\hat{M} = \text{diag}(M_u, M_d, M_s)$  with

$$\begin{aligned} M_u &= m_u - 4G_s(\Phi)\sigma_u + 2K(T)\sigma_d\sigma_s, \\ M_d &= m_d - 4G_s(\Phi)\sigma_d + 2K(T)\sigma_s\sigma_u, \\ M_s &= m_s - 4G_s(\Phi)\sigma_s + 2K(T)\sigma_u\sigma_d, \end{aligned}$$

and  $\sigma_f$  means the chiral condensate  $\langle \bar{\psi}_f \psi_f \rangle$  for flavor  $f$ . The mesonic potential  $U_M$  is

$$U_M = 2G_s(\Phi)(\sigma_u^2 + \sigma_d^2 + \sigma_s^2) - 4K(T)\sigma_u\sigma_d\sigma_s.$$

Making the path integral over quark fields, one can get the thermodynamic potential (per unit volume) as

$$\begin{aligned} \Omega = & U_M + \mathcal{U} - 2 \sum_{f=u,d,s} \int \frac{d^3\mathbf{p}}{(2\pi)^3} \left[ 3E_{p,f} \right. \\ & + \frac{1}{\beta} \ln [1 + 3(\Phi + \bar{\Phi}e^{-\beta E_{p,f}})e^{-\beta E_{p,f}} + e^{-3\beta E_{p,f}}] \\ & \left. + \frac{1}{\beta} \ln [1 + 3(\bar{\Phi} + \Phi e^{-\beta E_{p,f}})e^{-\beta E_{p,f}} + e^{-3\beta E_{p,f}}] \right] \end{aligned} \quad (10)$$

with  $E_{p,f} = \sqrt{\mathbf{p}^2 + M_f^2}$  and  $\beta = 1/T$ . We determine the mean-field variables ( $X = \sigma_l, \sigma_s, \Phi, \bar{\Phi}$ ) from the stationary conditions:

$$\frac{\partial \Omega}{\partial X} = 0, \quad (11)$$

where isospin symmetry is assumed for the light-quark sector, i.e.,  $\sigma_l \equiv \sigma_u = \sigma_d$ .

On the right-hand side of (10), the first term (vacuum term) in the momentum integral diverges. We then use the PV regularization [51, 52]. In the scheme, the integral  $I(M_f, q)$  is regularized as

$$I^{\text{reg}}(M_f, q) = \sum_{\alpha=0}^2 C_\alpha I(M_{f;\alpha}, q), \quad (12)$$

where  $M_{f;0} = M_f$  and the  $M_{f;\alpha}$  ( $\alpha \geq 1$ ) mean masses of auxiliary particles. The parameters  $M_{f;\alpha}$  and  $C_\alpha$  should satisfy the condition  $\sum_{\alpha=0}^2 C_\alpha = \sum_{\alpha=0}^2 C_\alpha M_{f;\alpha}^2 = 0$ . We then assume  $(C_0, C_1, C_2) = (1, 1, -2)$  and  $(M_{f;1}^2, M_{f;2}^2) = (M_f^2 + 2\Lambda^2, M_f^2 + \Lambda^2)$ . We keep the parameter  $\Lambda$  finite even after the subtraction (12), since the present model is non-renormalizable. The parameters are taken from Ref. [54] and they are  $m_l = 6.2$  MeV,  $m_s = 175.0$  MeV,  $G_s(0)\Lambda^2 = 2.35$  and  $K(0)\Lambda^5 = 27.8$  for  $\Lambda = 795$  MeV. This parameter set reproduces mesonic observables at vacuum, i.e., the pion and kaon decay constants ( $f_\pi = 92$  MeV and  $f_K = 105$  MeV) and their masses ( $M_\pi = 141$  MeV and  $M_K = 512$  MeV) and the  $\eta'$ -meson mass ( $M_{\eta'} = 920$  MeV). In the present work, we analyze LQCD results of Ref. [23] for pion and  $a_0$ -meson screening masses. In the LQCD simulation, the pion mass  $M_\pi(0)$  at vacuum ( $T = 0$ ) is 175 MeV and a bit heavier than the experimental value 138 MeV. We then change  $m_l$  to 9.9 MeV in the EPNJL model in order to reproduce  $M_\pi(0) = 175$  MeV. This parameter set yields  $M_{a_0}(0) = 711$  MeV,  $M_\eta(0) = 481$  MeV and  $M_\sigma(0) = 537$  MeV as  $a_0, \eta$  and  $\sigma$  meson pole masses at vacuum.

## B. Meson pole mass

We derive the equations for pion and  $a_0$ -meson pole masses, following Ref [36, 55]. The current corresponding to a meson of type  $\xi$  is

$$J_\xi(x) = \bar{\psi}(x) \Gamma_\xi \psi(x) - \langle \bar{\psi}(x) \Gamma_\xi \psi(x) \rangle, \quad (13)$$

where  $\Gamma_\pi = i\gamma_5 \lambda_3$  for  $\pi$  meson and  $\Gamma_{a_0} = \lambda_3$  for  $a_0$ -meson. We denote the Fourier transform of the mesonic correlation function  $\eta_{\xi\xi}(x) \equiv \langle 0 | T (J_\xi(x) J_\xi^\dagger(0)) | 0 \rangle$  by  $\chi_{\xi\xi}(q^2)$  as

$$\chi_{\xi\xi}(q^2) = \chi_{\xi\xi}(q_0^2, \tilde{q}^2) = i \int d^4x e^{iq \cdot x} \eta_{\xi\xi}(x), \quad (14)$$

where  $\tilde{q} = \pm|\mathbf{q}|$  for  $q = (q_0, \mathbf{q})$  and  $T$  stands for the time-ordered product. Using the random-phase (ring) approximation, one can obtain the Schwinger-Dyson equation

$$\chi_{\xi\xi} = \Pi_{\xi\xi} + 2 \sum_{\xi'\xi''} \Pi_{\xi\xi'} G_{\xi'\xi''} \chi_{\xi''\xi} \quad (15)$$

for  $\chi_{\xi\xi}$ , where  $G_{\xi'\xi''}$  is an effective four-quark interaction and  $\Pi_{\xi\xi'}$  is the one-loop polarization function defined by

$$\Pi_{\xi\xi'}(q^2) \equiv (-i) \int \frac{d^4p}{(2\pi)^4} \text{Tr} (\Gamma_\xi iS(p'+q) \Gamma_{\xi'} iS(p')) \quad (16)$$

with  $p' = (p_0 + iA_d, \mathbf{p})$ , where the trace  $\text{Tr}$  is taken in flavor, Dirac and color spaces. Here the quark propagator  $S(p)$  in momentum space is diagonal in flavor space:  $S(p) = \text{diag}(S_u, S_d, S_s)$ . For  $\xi = \pi$  and  $a_0$ , furthermore,  $G_{\xi\xi'}$  and  $\Pi_{\xi\xi'}$  are diagonal ( $G_{\xi\xi'} = G_\xi \delta_{\xi\xi'}$ ,  $\Pi_{\xi\xi'} = \Pi_\xi \delta_{\xi\xi'}$ ), because we impose isospin symmetry for the light-quark sector and employ the random-phase approximation. One can then easily solve the Schwinger-Dyson equation for  $\xi = \pi$  and  $a_0$ :

$$\chi_{\xi\xi} = \frac{\Pi_\xi}{1 - 2G_\xi \Pi_\xi} \quad (17)$$

with the effective couplings  $G_\pi$  and  $G_{a_0}$  defined by

$$G_{a_0} = G_s(\Phi) + \frac{1}{2} K(T) \sigma_s, \quad (18)$$

$$G_\pi = G_s(\Phi) - \frac{1}{2} K(T) \sigma_s. \quad (19)$$

As for  $T = 0$ ,  $\Pi_\pi$  and  $\Pi_{a_0}$  have the following explicit forms:

$$\begin{aligned} \Pi_{a_0} &= i \sum_{f,f'} (\lambda_3)_{f'f} (\lambda_3)_{ff'} \\ &\times \int \frac{d^4p}{(2\pi)^4} \text{tr}_{c,d} \left[ \frac{\{\gamma_\mu(p'+q)^\mu + M_f\} (\gamma_\nu p'^\nu + M_{f'})}{\{(p'+q)^2 - M_f^2\} (p'^2 - M_{f'}^2)} \right] \\ &= 4i[I_1 + I_2 - (q^2 - 4M^2)I_3], \end{aligned} \quad (20)$$

$$\begin{aligned} \Pi_\pi &= i \sum_{f,f'} (\lambda_3)_{f'f} (\lambda_3)_{ff'} \\ &\times \int \frac{d^4p}{(2\pi)^4} \text{tr}_{c,d} \left[ (i\gamma_5) \frac{\{\gamma_\mu(p'+q)^\mu + M_f\}}{\{(p'+q)^2 - M_f^2\}} \right. \\ &\quad \left. \times (i\gamma_5) \frac{(\gamma_\nu p'^\nu + M_{f'})}{(p'^2 - M_{f'}^2)} \right] \\ &= 4i[I_1 + I_2 - q^2 I_3], \end{aligned} \quad (21)$$

and

$$I_1 = \int \frac{d^4p}{(2\pi)^4} \text{tr}_c \left[ \frac{1}{p'^2 - M} \right], \quad (22)$$

$$I_2 = \int \frac{d^4p}{(2\pi)^4} \text{tr}_c \left[ \frac{1}{(p'+q)^2 - M^2} \right], \quad (23)$$

$$I_3 = \int \frac{d^4p}{(2\pi)^4} \text{tr}_c \left[ \frac{1}{\{(p'+q)^2 - M^2\} (p'^2 - M^2)} \right], \quad (24)$$

where  $\text{tr}_{c,d}$  ( $\text{tr}_c$ ) means the trace in color and Dirac spaces (color space) and  $M = M_u = M_d$ . For finite  $T$ , the corresponding equations are obtained by the replacement

$$\begin{aligned} p_0 &\rightarrow i\omega_n = i(2n+1)\pi T, \\ \int \frac{d^4p}{(2\pi)^4} &\rightarrow iT \sum_{n=-\infty}^{\infty} \int \frac{d^3\mathbf{p}}{(2\pi)^3}. \end{aligned} \quad (25)$$

The meson pole mass  $M_{\xi,\text{pole}}$  is a pole of  $\chi_{\xi\xi}(q_0^2, \tilde{q}^2)$  in the complex  $q_0$  plane. Taking the rest frame  $q = (q_0, \mathbf{0})$  for convenience, one can get the equation for  $M_{\xi,\text{pole}}$  as

$$[1 - 2G_\xi \Pi_\xi(q_0^2, 0)] \Big|_{q_0=M_{\xi,\text{pole}}-i\frac{\Gamma}{2}} = 0, \quad (26)$$

where  $\Gamma$  is the decay width to  $q\bar{q}$  continuum. The method of calculating meson pole masses is well established in the PNJL model [36, 55].

### C. Meson screening mass

We derive the equations for pion and  $a_0$ -meson screening masses, following Ref. [49]. This is an extension of the method of Ref. [49] for 2 flavors to 2+1 flavors.

As mentioned in Sec. I, it is not easy to make the Fourier transform from  $\chi_{\xi\xi}(0, \tilde{q}^2)$  to  $\eta_{\xi\xi}(r)$  particularly at large  $r$ . When the direct integration on the real  $\tilde{q}$  axis is difficult, one can consider a contour integral in the complex  $\tilde{q}$  plane by using the Cauchy's integral theorem. However,  $\chi_{\xi\xi}(0, \tilde{q}^2)$  has logarithmic cuts in the vicinity of the real  $\tilde{q}$  axis [51], and it is reported in Ref. [51] that heavy numerical calculations are necessary for evaluating the cut effects. In our previous work [49], we showed that these logarithmic cuts are unphysical and removable. Actually, we have no logarithmic cut, when analytic continuation is made for the  $I_3(\mathbf{q})$  after  $\mathbf{p}$  integration. Namely, the Matsubara summation over  $n$  should be taken after the  $\mathbf{p}$  integration in (25). We then express  $I_3^{\text{reg}}$  as an infinite series of analytic functions:

$$\begin{aligned} I_3^{\text{reg}}(0, \tilde{q}^2) &= iT \sum_{j=1}^{N_c} \sum_{n=-\infty}^{\infty} \sum_{\alpha=0}^2 C_\alpha \\ &\times \int \frac{d^3\mathbf{p}}{(2\pi)^3} \left[ \frac{1}{\mathbf{p}^2 + M_{j,n,\alpha}^2} \frac{1}{(\mathbf{p} + \mathbf{q})^2 + M_{j,n,\alpha}^2} \right] \\ &= \frac{iT}{2\pi^2} \sum_{j,n,\alpha} C_\alpha \int_0^1 dx \int_0^\infty dk \frac{k^2}{[k^2 + (x-x^2)\tilde{q}^2 + M_{j,n,\alpha}^2]^2} \\ &= \frac{iT}{4\pi\tilde{q}} \sum_{j,n,\alpha} C_\alpha \sin^{-1} \left( \frac{\frac{\tilde{q}}{2}}{\sqrt{\frac{\tilde{q}^2}{4} + M_{j,n,\alpha}^2}} \right) \end{aligned} \quad (27)$$

with

$$M_{j,n,\alpha}(T) = \sqrt{M_\alpha^2 + \{(2n+1)\pi T + A_4^{jj}\}^2}, \quad (28)$$

where  $M_\alpha = M_{u;\alpha} = M_{d;\alpha}$ . We have numerically confirmed that the convergence of  $n$ -summation is quite fast in (27). Each term of  $I_3^{\text{reg}}(0, \tilde{q}^2)$  has two physical cuts on the imaginary axis, one is an upward vertical line starting from  $\tilde{q} = 2iM_{j,n,\alpha}$  and the other is a downward vertical line from  $\tilde{q} = -2iM_{j,n,\alpha}$ . The lowest branch point is  $\tilde{q} = 2iM_{j=1,n=0,\alpha=0}$ . The value is the meson screening mass in which there is no interaction between a quark and an anti-quark, i.e.,  $G_\xi = 0$ . Hence we may call  $2M_{j=1,n=0,\alpha=0}$  "the threshold mass".

We can obtain the meson screening mass  $M_{\xi,\text{scr}}$  as a pole of  $\chi_{\xi\xi}(0, \tilde{q}^2)$ ,

$$\left[ 1 - 2G_\xi \Pi_\xi(0, \tilde{q}^2) \right] \Big|_{\tilde{q}=iM_{\xi,\text{scr}}} = 0. \quad (29)$$

If the pole at  $\tilde{q} = iM_{\xi,\text{scr}}$  is well isolated from the cut, i.e.,  $M_{\xi,\text{scr}} < 2M_{j=1,n=0,\alpha=0}$ , one can determine the screening mass from the pole location without making the  $\tilde{q}$  integral. In the high- $T$  limit, the condition tends to  $M_{\xi,\text{scr}} < 2\pi T$ .

### D. Meson susceptibility

We consider meson susceptibilities  $\chi_\xi^{\text{sus}}$  for  $\xi = \pi, a_0, \eta$  and  $\sigma$ . In LQCD simulations of Refs. [24, 25], the  $\chi_\xi^{\text{sus}}$  are defined in Euclidean spacetime  $x_E = (\tau, \mathbf{x})$  as

$$\chi_\xi^{\text{sus}} = \frac{1}{2} \int d^4x_E \langle J_\xi(\tau, \mathbf{x}) J_\xi^\dagger(0, \mathbf{0}) \rangle. \quad (30)$$

In the simulations,  $J_\sigma$  and  $J_\eta$  are assumed to have no s-quark component for simplicity: namely,  $J_\sigma = \sum_{f=u,d} \bar{\psi}_f \psi_f - \langle \sum_{f=u,d} \bar{\psi}_f \psi_f \rangle$  and  $J_\eta = \sum_{f=u,d} \bar{\psi}_f i\gamma_5 \psi_f - \langle \sum_{f=u,d} \bar{\psi}_f i\gamma_5 \psi_f \rangle$ . For consistency, we take the same assumption also in the present analysis, and denote the mesons with no s-quark (ns) component by  $\sigma_{\text{ns}}$  and  $\eta_{\text{ns}}$ . The factor 1/2 is introduced to define the  $\chi_\xi^{\text{sus}}$  as single-flavor quantities.

The  $\chi_\xi^{\text{sus}}$  is related to the Matsubara Green's function  $\chi_{\xi\xi}^E(q_4^2, \mathbf{q}^2)$  in the momentum representation as

$$\chi_\xi^{\text{sus}} = \frac{1}{2} \chi_{\xi\xi}^E(q_4^2, \mathbf{q}^2) \Big|_{q_4=0, \mathbf{q}=0}, \quad (31)$$

and  $\chi_{\xi\xi}^E$  is obtainable from (17) for  $\pi$  and  $a_0$  mesons. For  $\eta_{\text{ns}}$  meson, we have to consider a mixing between  $\eta_{\text{ns}}$  and  $\eta_s = \bar{\psi}_s i\gamma_5 \psi_s$ . As a result, one can obtain  $\chi_{\eta_{\text{ns}}\eta_{\text{ns}}}$  as [55]

$$\chi_{\eta_{\text{ns}}\eta_{\text{ns}}} = \frac{(1 - 2G_{\eta_s\eta_s} \Pi_{\eta_s\eta_s}) \Pi_{\eta_{\text{ns}}\eta_{\text{ns}}}}{\det[\mathbf{I} - 2\mathbf{G}\Pi]}, \quad (32)$$

where  $\mathbf{I}$  is the unit matrix and

$$\mathbf{G} = \begin{pmatrix} G_{\eta_s\eta_s} & G_{\eta_s\eta_{\text{ns}}} \\ G_{\eta_{\text{ns}}\eta_s} & G_{\eta_{\text{ns}}\eta_{\text{ns}}} \end{pmatrix}, \quad \mathbf{\Pi} = \begin{pmatrix} \Pi_{\eta_s\eta_s} & 0 \\ 0 & \Pi_{\eta_{\text{ns}}\eta_{\text{ns}}} \end{pmatrix} \quad (33)$$

for the elements

$$G_{\eta_s\eta_s} = G_s(\Phi), \quad (34)$$

$$G_{\eta_{\text{ns}}\eta_{\text{ns}}} = G_s(\Phi) + \frac{1}{2} K(T) \sigma_s, \quad (35)$$

$$G_{\eta_s\eta_{\text{ns}}} = G_{\eta_{\text{ns}}\eta_s} = \frac{\sqrt{2}}{2} K(T) \sigma_l. \quad (36)$$

In the isospin symmetric case we consider, the polarization functions  $\Pi_{\eta_s\eta_s}$  and  $\Pi_{\eta_{\text{ns}}\eta_{\text{ns}}}$  have the same function form as  $\Pi_\pi$ :

$$\Pi_{\eta_s\eta_s} = \Pi_\pi(M_s), \quad (37)$$

$$\Pi_{\eta_{\text{ns}}\eta_{\text{ns}}} = \Pi_\pi(M), \quad (38)$$

where note that  $\Pi_\pi(M_s)$  is a function of not  $M$  but  $M_s$ . Similarly,  $\chi_{\sigma_{\text{ns}}\sigma_{\text{ns}}}$  is obtainable from (32) with  $K(T)$  replaced by  $-K(T)$  and  $\Pi_\pi$  by  $\Pi_{a_0}$ .

## III. NUMERICAL RESULTS

### A. Meson screening masses

The EPNJL model has three adjustable parameters,  $\alpha_1$  in the entanglement coupling  $G_s(\Phi)$  and  $b$  and  $T_1$  in the KMT

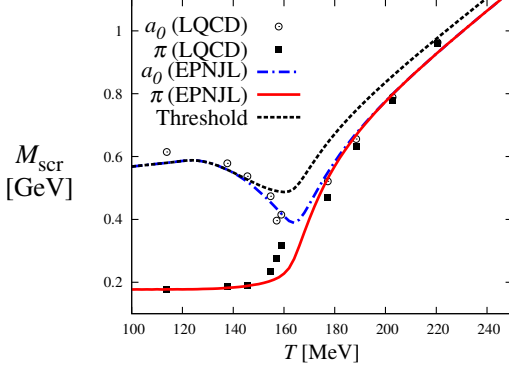


Fig. 2:  $T$  dependence of pion and  $a_0$ -meson screening masses,  $M_{\pi,\text{scr}}$  and  $M_{a_0,\text{scr}}$ . The solid (dot-dash) line denotes  $M_{\pi,\text{scr}}$  ( $M_{a_0,\text{scr}}$ ) calculated by the EPNJL model, whereas the dotted line corresponds to the threshold mass. LQCD data are taken from Ref. [23]; closed squares (open circles) correspond to the 2+1 flavor data for  $M_{\pi,\text{scr}}$  ( $M_{a_0,\text{scr}}$ ). In Ref. [23],  $T_c$  was considered 196 MeV, but it was refined to  $154 \pm 9$  MeV [5, 6]. The latest value is taken in this figure.

interaction  $K(T)$ . These parameters can be clearly determined from LQCD data [23] for pion and  $a_0$ -meson screening masses,  $M_{\pi,\text{scr}}$  and  $M_{a_0,\text{scr}}$ , as shown below.

Figure 2 shows  $T$  dependence of  $M_{\pi,\text{scr}}$  and  $M_{a_0,\text{scr}}$ . Best fitting is obtained, when  $\alpha_1 = 1.0$ ,  $T_1 = 0.79T_c = 121$  MeV and  $b = 0.23T_c = 36$  MeV. Actually, the EPNJL results (solid and dot-dash lines) with this parameter set well account for LQCD data [23] for both  $M_{\pi,\text{scr}}$  and  $M_{a_0,\text{scr}}$ . The parameters thus obtained indicate the strong suppression of  $K(T)$  in the vicinity of  $T_c$ . The mass difference  $\Delta M_{\text{scr}}(T) = M_{a_0,\text{scr}}(T) - M_{\pi,\text{scr}}(T)$  is sensitive to  $K(T)$  because of (18) and (19), and hence the values of  $b$  and  $T_1$  are well determined from  $\Delta M_{\text{scr}}(T)$ .

When  $\alpha_1 = 0$ , the EPNJL model is reduced to the PNJL model. The results of the PNJL model are shown in Fig. 3 for comparison. The PNJL results cannot reproduce LQCD data particularly in the region  $T \gtrsim 180$  MeV. The slope of the solid and dot-dash lines in the region is thus sensitive to the value of  $\alpha_1$ . Namely, the value of  $\alpha_1$  is well determined from the slope.

In Fig. 2, the solid and dot-dash lines are lower than the threshold mass  $2M_{j=1,n=0,\alpha=0}$  (dotted line). This guarantees that the  $M_{\pi,\text{scr}}$  and  $M_{a_0,\text{scr}}$  determined from the pole location in the complex- $\tilde{q}$  plane agree with those from the exponential decay of  $\eta_{\xi\xi}(r)$  at large  $r$ .

In the EPNJL model with the present parameter, the chiral susceptibility  $\chi_{ll}$  for light quarks has a peak at  $T = 163$  MeV, as shown later in Fig. 11(a). This indicates  $T_c = 163$  MeV. The model result is consistent with LQCD data  $T_c = 154 \pm 9$  MeV of Refs. [5, 6]. For the deconfinement transition, meanwhile, the parameter  $T_0$  is adjusted to reproduce LQCD data on  $T_c^{\text{deconf}}$ , as already mentioned in Sec. II. In fact, the Polyakov-loop susceptibility  $\bar{\chi}_{\Phi\bar{\Phi}}$  has a peak at  $T = 165$  MeV in the EPNJL model, as shown in Fig. 11(b). The model result  $T_c^{\text{deconf}} = 165$  MeV is consistent with LQCD data

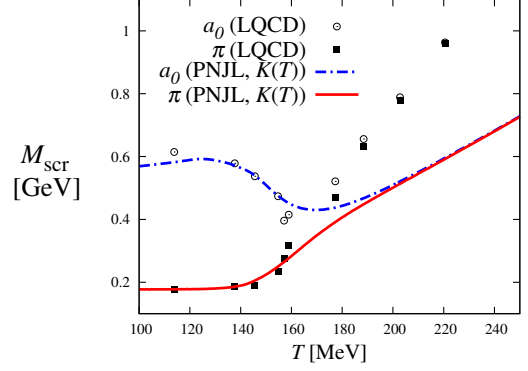


Fig. 3: Effects of  $T$ -dependent KMT interaction on pion and  $a_0$ -meson screening masses. The solid (dot-dash) line denotes  $M_{\pi,\text{scr}}$  ( $M_{a_0,\text{scr}}$ ) calculated by the PNJL model with  $T$ -dependent coupling  $K(T)$ . See Fig. 2 for LQCD data.

$T_c^{\text{deconf}} = 170 \pm 7$  MeV of Ref. [53].

Figure 4 shows  $T$  dependence of the renormalized chiral condensate  $\Delta_{l,s}$  defined by

$$\Delta_{l,s} \equiv \frac{\sigma_l(T) - \frac{m_l}{m_s} \sigma_s(T)}{\sigma_l(0) - \frac{m_l}{m_s} \sigma_s(0)}, \quad (39)$$

and the Polyakov loop  $\Phi$ . The present EPNJL model well reproduces LQCD data [5] for the magnitude of  $\Delta_{l,s}$  in addition to the value of  $T_c$ . The present model overestimates LQCD data for the magnitude of  $\Phi$ , although it yields a result consistent with LQCD for  $T_c^{\text{deconf}}$ . The overestimation in the magnitude of  $\Phi$  is a famous problem in the PNJL model. Actually, many PNJL calculations have this overestimation. This is considered to come from the fact that the definition of the Polyakov loop is different between LQCD and the PNJL model [56, 57]. In LQCD the definition is  $\Phi_{\text{LQCD}} = \langle \text{tr}_c \mathcal{P} \exp[i \int_0^{1/T} d\tau A_4(\tau, \mathbf{x})] \rangle / 3$ , while in the PNJL model based on the Polyakov gauge and the mean field approximation the definition is  $\Phi_{\text{PNJL}} = \text{tr}_c \exp[i \langle A_4 \rangle / T] / 3$ , although both are order parameters of  $Z_3$  symmetry [56, 57]; see for example Ref. [31, 58] as a trial to solve this problem.

Now we investigate effects of  $T$ -dependent KMT interaction  $K(T)$  on  $M_{\pi,\text{scr}}$  and  $M_{a_0,\text{scr}}$ . In Fig. 5,  $T$ -dependence of  $K(T)$  is switched off; namely, results of the EPNJL model with  $K(T) = K(0)$  are shown. One can see that  $T$ -dependence of  $K(T)$  reduces the mass difference between  $M_{\pi,\text{scr}}$  and  $M_{a_0,\text{scr}}$  significantly in a range  $150 \lesssim T \lesssim 180$  MeV, comparing Fig. 5 with Fig. 2. At  $T = 176$  MeV where first-order chiral and deconfinement transitions take place,  $M_{\pi,\text{scr}}$  has a jump while  $M_{a_0,\text{scr}}$  has a cusp. Meson screening mass is thus a good indicator for a first-order transition.

In Fig. 6, both the  $T$  dependence of  $K(T)$  and the entanglement of  $G_s(\Phi)$  are switched off. Namely, the results of the standard PNJL model with a constant  $K$  are shown. The model cannot reproduce LQCD data, as expected.

Figure 7 shows three types of EPNJL calculations for the mass difference  $\Delta M_{\text{scr}}(T)$ . The mass difference plays a role

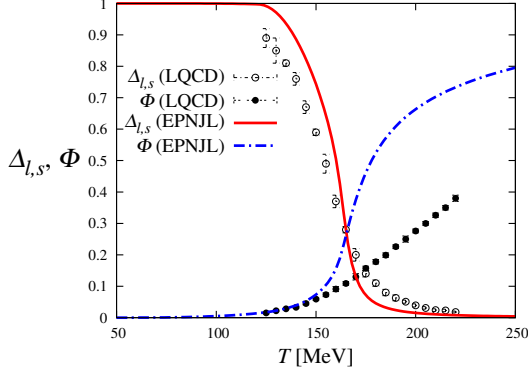


Fig. 4:  $T$  dependence of  $\Delta_{l,s}$  and  $\Phi$ . The solid (dot-dash) line corresponds to results of the EPNJL model for  $\Delta_{l,s}$  ( $\Phi$ ). LQCD data for 2+1 flavors are taken from Ref. [5].

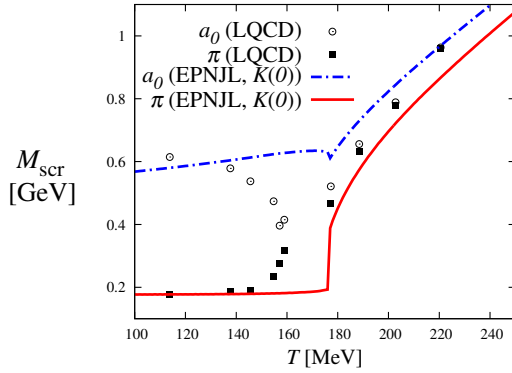


Fig. 5: Effects of  $T$ -dependent KMT interaction on pion and  $a_0$ -meson screening masses. The solid (dot-dash) line denotes  $M_{\pi,scr}$  ( $M_{a_0,scr}$ ) calculated by the EPNJL model with  $K(T) = K(0)$ . See Fig. 2 for LQCD data.

of the order parameter of the effective restoration of  $U(1)_A$ . The full-fledged EPNJL calculation (solid line) with both  $T$ -dependent  $K$  and the entanglement coupling  $G_s(\Phi)$  well reproduces LQCD data, while the standard PNJL model (dotted line) with constant  $K$  largely overestimates the data.

The present model has  $T$  dependence implicitly in  $G_s(\Phi)$  through  $\Phi$  and explicitly in  $K(T)$ . As a model opposite to the present one, one may consider the case that  $K(T) = K(0)$  and  $G_s$  has  $T$  dependence explicitly, i. e.,  $G_s = G_s(T)$ . We can determine  $G_s(T)$  so as to reproduce LQCD data for  $\Delta_{l,s}$ , however, this model overestimates LQCD data for  $\Delta M_{scr}$ . Thus the present model is well designed.

## B. Meson susceptibilities

The validity of  $K(T)$  is investigated by comparing LQCD data with the model results for meson susceptibilities  $\chi_\xi^{\text{sus}}$  ( $\xi = \pi, a_0, \eta_{\text{ns}}, \sigma_{\text{ns}}$ ). LQCD data based on domain-wall fermions [25] are available for two cases of pion mass  $M_\pi(0)$

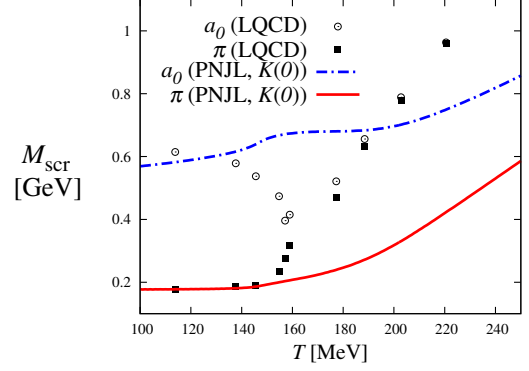


Fig. 6: Effects of the entanglement coupling  $G_s(\Phi)$  on pion and  $a_0$ -meson screening masses. The solid (dot-dash) line denotes  $M_{\pi,scr}$  ( $M_{a_0,scr}$ ) calculated by the standard PNJL model with constant  $K$ , i.e., the EPNJL model with  $K(T) = K(0)$  and  $\alpha_1 = 0$ . See Fig. 2 for LQCD data.

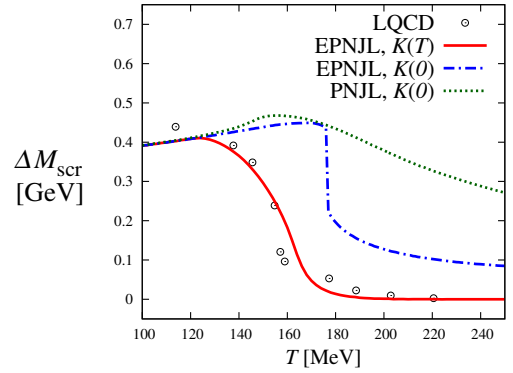


Fig. 7: Mass difference  $\Delta M_{scr}(T)$  between pion and  $a_0$ -meson screening masses. The solid, dot-dash and dotted lines denote results of the EPNJL model, the EPNJL model with  $K(T) = K(0)$  and the standard PNJL model with  $K(T) = K(0)$ , respectively. See Fig. 2 for LQCD data.

at vacuum being the physical value 135 MeV and a slightly heavier value 200 MeV. In order to reproduce these values with the EPNJL model, we take  $m_l = 5.68$  MeV for the first case and 12.8 MeV for the second one.

We consider the difference  $\Delta_{\pi,a_0} = \chi_\pi^{\text{sus}} - \chi_{a_0}^{\text{sus}}$  as an order parameter of the effective  $U(1)_A$ -symmetry restoration. Figure 8 shows  $T$  dependence of  $\Delta_{\pi,a_0}/T^2$  for two cases of  $M_\pi(0) = 135$  and 200 MeV. Since the  $\chi_\xi^{\text{sus}}$  have ultraviolet divergence, they are renormalized with the  $\overline{\text{MS}}$  scheme in LQCD. For this reason, one cannot compare the LQCD data with the results of the EPNJL model directly. We then multiply the model results by a constant so as to reproduce LQCD data at  $T = 139$  MeV for the case of  $M_\pi(0) = 135$  MeV. The model results thus renormalized well reproduce LQCD data for any  $T$  in both cases of  $M_\pi(0) = 135$  and 200 MeV.

A similar analysis is made for  $T$  dependence of  $\Delta_{\pi,\sigma} = \chi_\pi^{\text{sus}} - \chi_{\sigma_{\text{ns}}}^{\text{sus}}$  and  $\Delta_{\eta,a_0} = \chi_{\eta_{\text{ns}}}^{\text{sus}} - \chi_{a_0}^{\text{sus}}$  that are related to

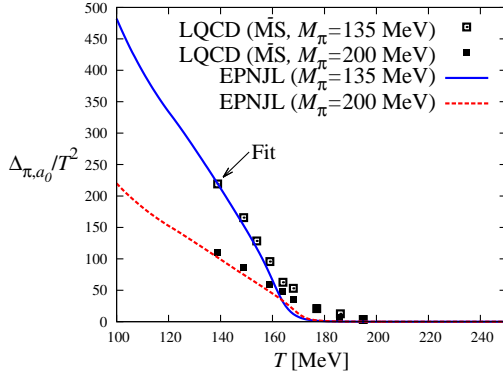


Fig. 8:  $T$  dependence of the difference  $\Delta_{\pi,a_0}$  between  $\pi$  and  $a_0$  meson susceptibilities for two cases of  $M_\pi(0) = 135$  and  $200$  MeV.

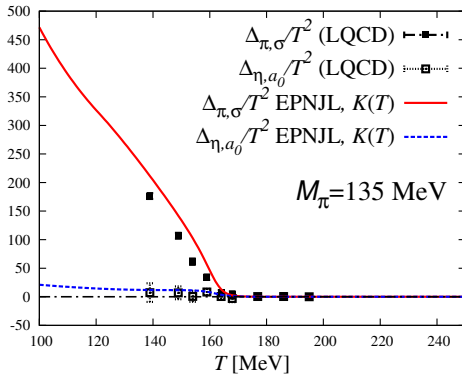


Fig. 9:  $T$  dependence of  $\Delta_{\pi,\sigma}$  and  $\Delta_{\eta,a_0}$  for  $M_\pi(0) = 135$  MeV.

$SU_L(2) \times SU_R(2)$  symmetry. Figure 9 (10) shows  $T$  dependence of  $\Delta_{\pi,\sigma}/T^2$  and  $\Delta_{\eta,a_0}/T^2$  for  $M_\pi(T) = 135$  (200) MeV. In both the figures, the EPNJL model well reproduces  $T$  dependence of LQCD results. The present model with the  $K(T)$  of (6) is thus reasonable.

### C. The order of chiral transition near the physical point

Finally we consider the order of chiral transition near the physical point  $(m_l^{\text{phys}}, m_s^{\text{phys}}) = (6.2[\text{MeV}], 175[\text{MeV}])$  in the  $m_l$ - $m_s$  plane, First we vary  $m_l$  from 9.9 to 0 MeV with  $m_s$  fixed at 175 MeV.

Figure 11 presents  $T$  dependence of the chiral susceptibility  $\chi_{ll}$  for light quarks and the Polyakov-loop susceptibility  $\bar{\chi}_{\phi\bar{\phi}}$  in three points, “simulation point (S-point)” of  $(m_l, m_s) = (9.9[\text{MeV}], 175[\text{MeV}])$ , “physical point (P-point)” of  $(m_l, m_s) = (6.2[\text{MeV}], 175[\text{MeV}])$  and “light-quark chiral-limit point (C<sub>l</sub> point)” of  $(m_l, m_s) = (0[\text{MeV}], 175[\text{MeV}])$ . In general,  $T_c$  and  $T_c^{\text{deconf}}$  determined from peak positions of  $\chi_{ll}$  and  $\bar{\chi}_{\phi\bar{\phi}}$  depend on  $m_l$  and  $m_s$ . However, as shown in panel (a), the  $T_c$  thus determined is 163 MeV at S-point and 160 MeV at P-point, and hence the

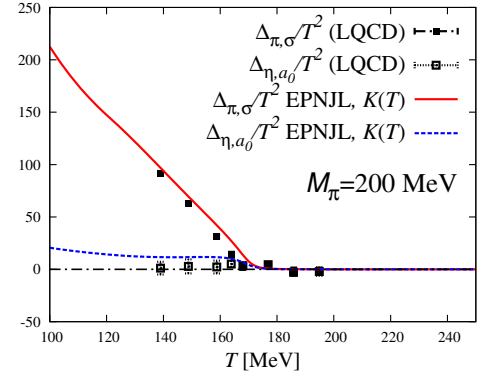


Fig. 10:  $T$  dependence of  $\Delta_{\pi,\sigma}$  and  $\Delta_{\eta,a_0}$  for  $M_\pi(0) = 200$  MeV.

value little varies between the two points. At C<sub>l</sub> point,  $\chi_{ll}$  diverges at  $T = T_c = 153$  MeV. The chiral transition is thus second order at C<sub>l</sub>-point at least in the mean-field level. This result suggests that the effective  $U(1)_A$  restoration is not completed at  $T = T_c$ . This suggestion is supported by LQCD data at S-point in Fig. 7 where  $\Delta M_{\text{scr}}(T_c)$  is about a half of  $\Delta M_{\text{scr}}(0)$ .

As shown in panel (b),  $m_l$  dependence of  $T_c^{\text{deconf}}$  is even smaller; namely,  $T_c^{\text{deconf}} = 165$  MeV for S-point and C<sub>l</sub>-point and 163 MeV for P-point. At C<sub>l</sub>-point,  $\bar{\chi}_{\phi\bar{\phi}}$  has a sharp peak at  $T = 153$  MeV. It is just a result of the propagation of divergence from  $\chi_{ll}$  to  $\bar{\chi}_{\phi\bar{\phi}}$  [59], and never means that a second-order deconfinement takes place there.

Next, both  $m_l$  and  $m_s$  are varied near P-point. Figure 12 shows the value of  $\log[\chi_{ll}(T_c)]$  near P-point in the  $m_l$ - $m_s$  plane. The value is denoted by a change in hue. Three second-order chiral transitions (solid lines) meet at  $(m_l^{\text{tric}}, m_s^{\text{tric}}) \approx (0, 0.726m_s^{\text{phys}}) = (0[\text{MeV}], 127[\text{MeV}])$ . This is a tricritical point (TCP) of chiral phase transition.

## IV. SUMMARY

In summary, we incorporated the effective restoration of  $U(1)_A$  symmetry in the 2+1 flavor EPNJL model by introducing a  $T$ -dependent coupling strength  $K(T)$  to the KMT interaction. The  $T$  dependence was well determined from state-of-the-art 2+1 flavor LQCD data on pion and  $a_0$ -meson screening masses. To derive the meson screening masses in the EPNJL model, we extended our previous prescription of Ref. [49] for 2 flavors to 2+1 flavors. The strength  $K(T)$  thus obtained is suppressed in the vicinity of the pseudocritical temperature of chiral transition. As a future work, it is quite interesting to clarify how the present suppression is explained by instantons.

In order to check the validity of  $K(T)$ , we analyze  $\pi$ ,  $a_0$ ,  $\eta_{\text{ns}}$ ,  $\sigma_{\text{ns}}$ -meson susceptibilities obtained by state-of-the-art LQCD simulations with domain-wall fermions [25]. The EPNJL model with the  $K(T)$  of (6) well reproduces  $T$  dependence of LQCD data. The present model building is thus reasonable.

Using the EPNJL model with the present parameter set,

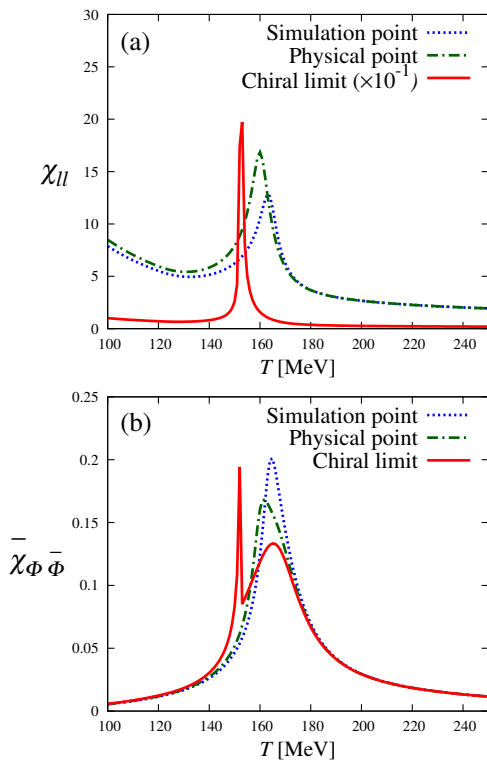


Fig. 11:  $T$  dependence of (a) chiral susceptibility  $\chi_u$  and (b) Polyakov-loop susceptibility  $\bar{\chi}_{\Phi\bar{\Phi}}$  at S-point, P-point and  $C_l$ -point. Here  $\chi_u$  and  $\bar{\chi}_{\Phi\bar{\Phi}}$  are dimensionless and their definition is the same as in the LQCD formulation. Calculations are done by the EPNJL model with the present parameter set. The dotted, dot-dash and solid lines stand for the results at S-point, P-point and  $C_l$ -point, respectively. At  $C_l$ -point,  $\chi_u$  is divided by 10 and diverges at  $T = T_c = 153$  MeV

we showed that, at least in the mean field level, the order of chiral transition is second order at the light-quark chiral-limit point of  $m_l = 0$  and  $m_s = 175$  MeV (the physical value). This result indicates that there exists a tricritical point near the light-quark chiral-limit point in the  $m_l$ - $m_s$  plane. We then estimated the location of the tricritical point as  $(m_l, m_s) \approx (0[\text{MeV}], 127[\text{MeV}])$ .

In conclusion, we present a simple method for calculating meson screening masses in PNJL-like models. This allows us to compare model results with LQCD data on meson screening masses. Meson screening masses are quite useful to determine model parameters. In particular, the mass difference

between pion and  $a_0$ -meson is effective to determine  $T$  dependence of the KMT interaction. The EPNJL model with the present parameter set is useful for estimating the order of chiral transition at the light-quark chiral-limit point and the location of the tricritical point, since it is hard to reach the chiral regime directly with LQCD.

The present model consists of  $\Phi$ -dependent four-quark interactions and  $T$ -dependent six-quark interactions. Meanwhile, the importance of eight-quark interactions was pointed out in Ref. [60], since it makes the thermodynamic potential

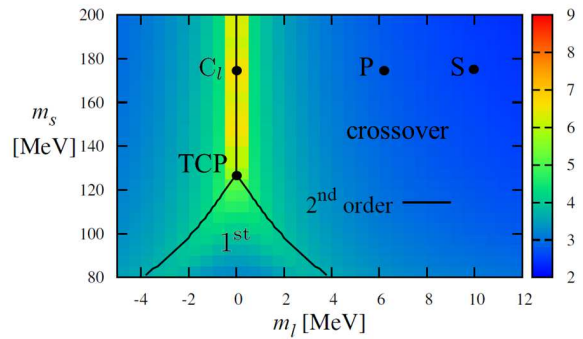


Fig. 12: Order of chiral transition near physical point in the  $m_l$ - $m_s$  plane. The value of  $\log[\chi_u(T_c)]$  is shown by a change in hue. Simulation point, physical point, light-quark chiral-limit point and tricritical point are denoted by S, P,  $C_l$  and TCP. The solid lines stand for second-order chiral transitions.

bounded from below. Furthermore, it is reported in Ref. [61] that current-quark-mass dependence of quark-quark interactions is effective to reproduce meson pole masses with good accuracy. Therefore, further inclusion of these interactions is interesting as a future work.

### Acknowledgments

M. I., J. T., H. K., and M. Y. are supported by Grant-in-Aid for Scientific Research (No. 27-3944, No. 25-3944, No. 26400279 and No. 26400278) from the Japan Society for the Promotion of Science (JSPS).

[1] M. Kobayashi, and T. Maskawa, Prog. Theor. Phys. **44**, 1422 (1970); M. Kobayashi, H. Kondo, and T. Maskawa, Prog. Theor. Phys. **45**, 1955 (1971).  
 [2] G. 't Hooft, Phys. Rev. Lett. **37**, 8 (1976); Phys. Rev. D **14**, 3432 (1976); **18**, 2199(E) (1978).  
 [3] R. D. Pisarski, and L. G. Yaffe, Phys. Lett. B **97**, 110 (1980).  
 [4] E. V. Shuryak, Comments Nucl. Part. Phys. **21**, 235 (1994)

[arXiv:9310253].  
 [5] S. Borsanyi *et al.*, J. High Energy Phys. 09 (2010) 073 [arXiv:1005.3508].  
 [6] A. Bazavov, T. Bhattacharya, M. Cheng, C. DeTar, H. -T. Ding, S. Gottlieb, R. Gupta, and P. Hegde *et al.*, Phys. Rev. D **85**, 054503 (2012) [arXiv: 1111.1710].  
 [7] K. Kanaya, [arXiv: 1012.4235]; [arXiv: 1012.4247].

- [8] R. D. Pisarski, and F. Wilczek, Phys. Rev. D **29**, 338(R) (1984).
- [9] E. Vicari, Proc. Sci., LATTICE2007 (**2007**) 23 [arXiv: 0709.1014].
- [10] A. Pelissetto, and E. Vicari, Phys. Rev. D **88**, 105018 (2013).
- [11] M. Fukugita, H. Mino, M. Okawa, and A. Ukawa, Phys. Rev. Lett. **65**, 816 (1990).
- [12] M. Fukugita, H. Mino, M. Okawa, and A. Ukawa, Phys. Rev. D **42**, 2936 (1990).
- [13] F. R. Brown, F. P. Butler, H. Chen, N. H. Christ, Z. Dong, W. Schaffer, L. I. Unger, and A. Vaccarino, Phys. Rev. Lett. **65**, 2491 (1990).
- [14] F. Karsch, Phys. Rev. D **49**, 3791 (1994).
- [15] F. Karsch, and E. Laermann, Phys. Rev. D **50**, 6954 (1994).
- [16] Y. Iwasaki, K. Kanaya, S. Kaya, and T. Yoshie, Phys. Rev. Lett. **78**, 179 (1997).
- [17] S. Aoki *et al.* (JLQCD Collaboration), Phys. Rev. D **57**, 3910 (1998).
- [18] A. A. Khan *et al.* (CP-PACS Collaboration), Phys. Rev. D **63**, 034502 (2000).
- [19] C. Bernard, C. DeTar, S. Gottlieb, U. M. Heller, J. Hetrick, K. Rummukainen, R. L. Sugar, and D. Toussaint, Phys. Rev. D **61**, 054503 (2000).
- [20] M. D'Elia, A. Di Giacomo, and C. Pica, Phys. Rev. D **72**, 114510 (2005).
- [21] S. Ejiri *et al.*, Phys. Rev. D **80**, 094505 (2009).
- [22] C. Bonati, P. de Forcrand, M. D'Elia, O. Philipsen, and F. Sanfilippo, Phys. Rev. D **90**, 074030 (2014).
- [23] M. Cheng, S. Datta, A. Francis, J. van der Heide, C. Jung, O. Kaczmarek, F. Karsch, and E. Laermann *et al.*, Eur. Phys. J. C **71**, 1564 (2011) [arXiv: 1010.1216].
- [24] M. I. Buchoff, M. Cheng, N. H. Christ, H. -T. Ding, C. Jung, F. Karsch, Z. Lin, and R. D. Mawhinney *et al.*, Phys. Rev. D **89**, 054514 (2014) [arXiv: 1309.4149].
- [25] T. Bhattacharya, M. I. Buchoff, N. H. Christ, H. -T. Ding, R. Gupta, C. Jung, F. Karsch, and Z. Lin *et al.*, Phys. Rev. Lett. **113**, 082001 (2014) [arXiv: 1402.5175].
- [26] P. N. Meisinger, and M. C. Ogilvie, Phys. Lett. B **379**, 163 (1996).
- [27] A. Dumitru, and R. D. Pisarski, Phys. Rev. D **66**, 096003 (2002).
- [28] K. Fukushima, Phys. Lett. B **591**, 277 (2004); K. Fukushima, Phys. Rev. D **77**, 114028 (2008); Phys. Rev. D **78**, 114019 (2008).
- [29] P. Costa, M. C. Ruivo, C. A. de Sousa, and Yu. L. Kalinovsky, Phys. Rev. D **71**, 116002 (2005).
- [30] S. K. Ghosh, T. K. Mukherjee, M. G. Mustafa, and R. Ray, Phys. Rev. D **73**, 114007 (2006).
- [31] E. Megías, E. R. Arriola, and L. L. Salcedo, Phys. Rev. D **74**, 065005 (2006).
- [32] C. Ratti, M. A. Thaler, and W. Weise, Phys. Rev. D **73**, 014019 (2006).
- [33] M. Ciminale, R. Gatto, G. Nardulli, and M. Ruggieri, Phys. Lett. B **657**, 64 (2007); M. Ciminale, R. Gatto, N. D. Ippolito, G. Nardulli, and M. Ruggieri, Phys. Rev. D **77**, 054023 (2008).
- [34] C. Ratti, S. Rößner, M. A. Thaler, and W. Weise, Eur. Phys. J. C **49**, 213 (2007).
- [35] S. Rößner, C. Ratti, and W. Weise, Phys. Rev. D **75**, 034007 (2007).
- [36] H. Hansen, W. M. Alberico, A. Beraudo, A. Molinari, M. Nardi, and C. Ratti, Phys. Rev. D **75**, 065004 (2007).
- [37] C. Sasaki, B. Friman, and K. Redlich, Phys. Rev. D **75**, 074013 (2007).
- [38] B. -J. Schaefer, J. M. Pawłowski, and J. Wambach, Phys. Rev. D **76**, 074023 (2007).
- [39] K. Kashiwa, H. Kouno, M. Matsuzaki, and M. Yahiro, Phys. Lett. B **662**, 26 (2008).
- [40] P. Costa, M. C. Ruivo, C. A. de Sousa, H. Hansen, and W. M. Alberico, Phys. Rev. D **79**, 116003 (2009).
- [41] M. C. Ruivo, M. Santos, P. Costa, and C. A. de Sousa, Phys. Rev. D **85**, 036001 (2012).
- [42] Y. Sakai, T. Sasaki, H. Kouno, and M. Yahiro, Phys. Rev. D **82**, 076003 (2010).
- [43] T. Sasaki, Y. Sakai, H. Kouno, and M. Yahiro, Phys. Rev. D **84**, 091901(R) (2011).
- [44] M. D'Elia, and F. Sanfilippo, Phys. Rev. D **80**, 111501(R) (2009).
- [45] P. de Forcrand, and O. Philipsen, Phys. Rev. Lett. **105**, 152001 (2010) [arXiv:1004.3144].
- [46] J. B. Kogut, and D. K. Sinclair, Phys. Rev. D **70**, 094501 (2004).
- [47] P. de Forcrand, and O. Philipsen, J. High Energy Phys. **01** (2007) 077.
- [48] M. C. Ruivo, P. Costa, and C. A. de Sousa, Phys. Rev. D **86**, 116007 (2012).
- [49] M. Ishii, T. Sasaki, K. Kashiwa, H. Kouno, and M. Yahiro, Phys. Rev. D **89**, 071901(R) (2014). [arXiv:1312.7424].
- [50] T. Kunihiro, Nucl. Phys. B **351**, 593 (1991).
- [51] W. Florkowski, Acta Phys. Pol. B **28**, 2079 (1997) [arXiv:9701223].
- [52] W. Pauli, and F. Villars, Rev. Mod. Phys. **21**, 434 (1949).
- [53] Y. Aoki, S. Borsányi, S. Dürr, Z. Fodor, S. D. Katz, S. Krieg, and K. K. Szabo, J. High Energy Phys. **06** (2009) 088 [arXiv:0903.4155].
- [54] V. Bernard, and D. Vautherin, Phys. Rev. D **40**, 1615 (1989).
- [55] S. P. Klevansky Rev. Mod. Phys. **64**, 649 (1992); T. Hatsuda, and T. Kunihiro Phys. Rep. **247**, 221 (1994); M. Buballa Phys. Rep. **407**, 205 (2005).
- [56] J. Braun, H. Gies, and J. M. Pawłowski, Phys. Lett. B **684**, 262 (2010) [arXiv:0708.2413].
- [57] F. Mårhauser, and J. M. Pawłowski, [arXiv:0812.1144].
- [58] E. R. Arriola, L. L. Salcedo, and E. Megías, Acta Phys. Pol. B **45**, 2407(2014) .
- [59] K. Kashiwa, M. Yahiro, H. Kouno, M. Matsuzaki, and Y. Sakai, J. Phys. G **36**, 105001 (2009).
- [60] A. A. Osipov, B. Hiller, V. Bernard, and A. H. Blin, Ann. Phys. **321** (2006) 2504.
- [61] A. A. Osipov, B. Hiller, and A. H. Blin, Phys. Rev. D **88**, 054032 (2013).